

A novel single step chemical route for noble metal nanoparticles embedded organic–inorganic composite films

Sangaraju Shanmugam, B. Viswanathan*, T.K. Varadarajan

Department of Chemistry, Indian Institute of Technology Madras, Chennai 600036, India

Received 19 March 2005; received in revised form 29 April 2005; accepted 26 May 2005

Abstract

A novel single step chemical route is described to embed the silver and gold nanoparticles in composite films. The embedded composite films were characterized with, UV–vis, TEM and XPS analysis. The sizes of the noble metal nanoparticles are in the range of 12–16 nm. Potential possibilities as antimicrobial coating against *Escherichia coli* is presented.

© 2005 Elsevier B.V. All rights reserved.

Keywords: Noble metal nanoparticles; Organic–inorganic nanocomposite; Silicotungstic acid; *E. coli*; Antimicrobial activity

1. Introduction

The nanoparticles of noble metals have found potential applications in various fields like microelectronics, optical, electronic [1] and catalytic properties [2]. There have been numerous recent reports to fabricate the nanoparticles in one-dimensional, two-dimensional nanostructured materials for controlling the shapes and particle sizes [3]. To realize the potentialities of noble metal nanoparticles in technological and biological applications, they should be entrapped/embedded in polymer matrix, these can be made into thin films or scaffolded. Polyoxometalates are metal oxide clusters, discrete and well defined at atomic level with extensive structures and properties [4]. Polyoxometalates with Keggin type structures undergo stepwise multielectron redox process without structural modification by electrochemical, photochemical or radiolytical means. Troupis et al. have employed polyoxometalates as photocatalysts and stabilizers to prepare noble metal nanoparticles in homogeneous medium [5]. Recently, similar synthetic strategies have been adopted to prepare Au–Ag core shell nanoparticles and gold nanosheets [6].

Aymonier et al. [7] have demonstrated that the encapsulation of silver nanoparticle in hyperbranched polymer, exhibits antimicrobial activity. Silver coated catheters prevented the adherence and growth of *Escherichia coli* and *Pseudomonas aeruginosa* in vitro without causing cell toxicity [8].

The embedded silver and gold nanoparticles in dielectric matrices have been reported and their non-linear optical properties were studied. Several approaches have been reported to embed the noble metal nanoparticles in various matrices, such as silica, alumina, borate glass and MgO by sputtering, ion implantation, thermal vapor deposition and radio frequency magnetron co-sputtering [9]. All these methods require tedious procedures to adopt.

In this communication, a single step soft chemical route is described to embed the silver and gold nanoparticles in organic–inorganic composite and their antimicrobial activity against *E. coli* is described. As such no reports are available at present for embedding the silver and gold nanoparticles in organic–inorganic composite by this strategy.

2. Experimental

The composite is synthesized by sol–gel method. For a typical synthesis, 1.5 g of polyvinyl alcohol (PVA 72000) was dissolved in 30 ml distilled water stirred for 30 min and 2.5 ml

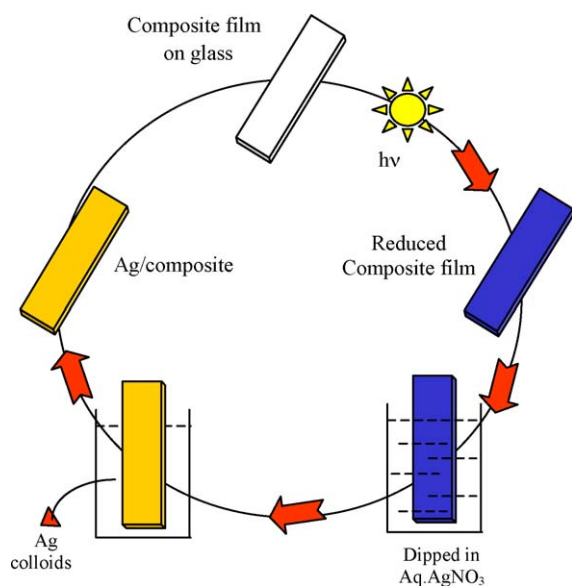
* Corresponding author. Tel.: +91 4422578250; fax: +91 4422578241.
E-mail address: bvnathan@iitm.ac.in (B. Viswanathan).

of tetraethyl orthosilicate (TEOS) was added and the mixture was stirred for 10 min, then 0.5 g of silicotungstic acid (SiW) was added and refluxed at 343 K for 6 h. The obtained gel was coated on glass slides by spin coating method and dried at room temperature.

3. Results and discussion

The photoreduction of silicotungstic acid was monitored through UV–vis spectroscopy, which showed a characteristic band around 750 nm indicating the formation of single electron reduced silicotungstate ion. Up to 60 min, with an increase in the irradiation time the intensity at 750 nm increased. After 60 min irradiation, there was no change in the intensity indicating that all the silicotungstate ions in the composite have been reduced. The ESR spectra of photoreduced composite film exhibited a signal at $g = 1.813$ at 77 K, which is due to the formation of single electron reduced species $\text{SiW}_{12}\text{O}_{40}^{5-}$ [10]. The reduced composite film is stable (retains blue colour) for longer times. The reduced composite was employed as reducing medium as well as host for the formation of metal nanoparticles. This reaction is truly heterogenous in nature. A typical preparation of embedded silver metal nanoparticles is shown in Scheme 1.

It is well known that the noble metal nanoparticles exhibits surface plasmons. So, the formation of metal nanoparticles in the composite film was monitored by UV–vis spectroscopy. The composite film after exposure to sunlight, which was dipped into a solution of AgNO_3 (20 mM) for 10 min and the corresponding absorption spectrum of the film is shown in Fig. 1. The blue colour of the film gradually changed to



Scheme 1. Preparation of noble metal nanoparticles embedded composite film.

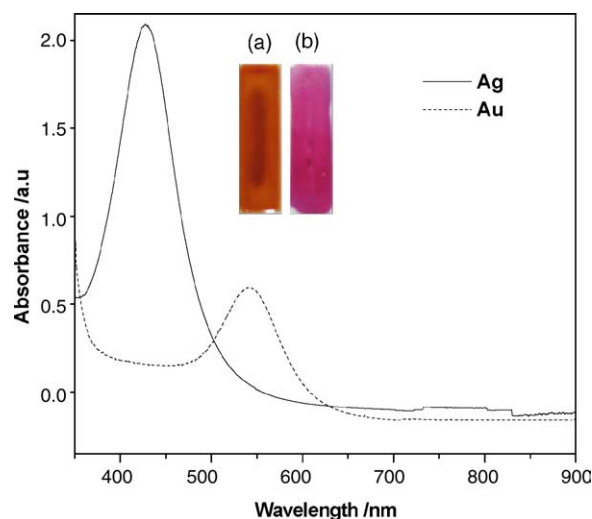


Fig. 1. Absorption spectra of noble metal nanoparticles embedded in composite films: (a) Ag and (b) Au. Inset shows the picture of Ag and Au embedded composite films.

yellow within a few minutes indicating the formation of Ag nanoparticles in the composite film. The Ag^+ ions from solution diffuse inside the film matrix where it is reduced to Ag metal nanoparticle and the silicotungstate ions are reoxidized. The embedded Ag nanoparticles exhibit the characteristic surface plasmon band at 427 nm (Fig. 1). The particle size can be controlled by dipping time intervals and concentration of metal ion solutions. A red shift of the surface plasmon band of Ag is evident from Fig. 2 as the dipping time is increased from 5 to 30 min with concomitant peak broadening. The shift to the higher wavelength and broadening of the surface plasmon absorption band upon incorporation of silver in the composite film is induced by the change in dielectric constant of the environment around the Ag nanoparticles [11]. As the concentration of AgNO_3 is increased, the intensity of the surface

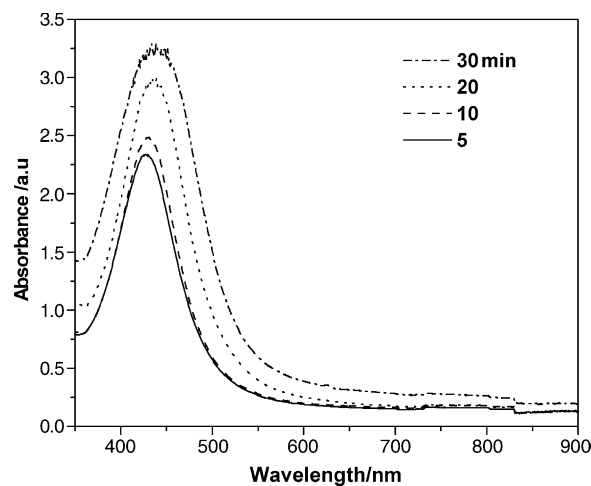


Fig. 2. UV–vis absorption spectra of Ag embedded composite film at different dipping time intervals, AgNO_3 20 mM.

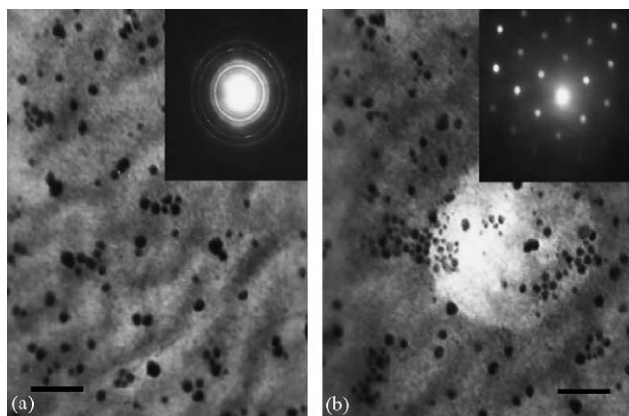


Fig. 3. Transmission electron micrographs of noble metal nanoparticles embedded composite films: (a) Ag and (b) Au. Insets show respective electron diffraction pattern. Scale bar 100 nm.

plasmon band increases and the absorption shifts to higher wavelength. The red shift and broadening of the surface plasmon band is due to the change in dielectric constant and also the increase in particle size and amount of metal nanoparticles in composite film. From the absorption spectra (Fig. 2), it is evidenced from full-width at half-maximum (FWHM), the particle size is increased as the dipping time increased [11]. The FWHM of the surface plasmon band is increased from 74 to 112 nm as the dipping time increases from 5 to 30 min. The FWHM of the peak is 112 nm for 30 min, which corresponds to 12 nm average diameter of embedded Ag nanoparticles. This is in good agreement with the TEM measurements. And also from the increase in surface plasmon band intensity indicates that the increase in amount of metal nanoparticles in composite film. The rate of formation of silver nanoparticles was calculated for 20 mM AgNO_3 and the rate constant was found to be $3.99 \times 10^{-3} \text{ s}^{-1}$. This is corroborated by the results obtained by Rodriguez-Sanchez et al. [12] and Haung et al. [13] for the formation of silver nanoparticles by electrochemical and chemical methods, respectively.

Similarly, Au nanoparticles were also embedded into the organic–inorganic composite films by dipping the reduced composite film in 5.4 mM aqueous solution of HAuCl_4 . The blue colour of the film changed into pink (inset, Fig. 1b) after 30 min dipping, showed a characteristic surface plasmon band at 546 nm (Fig. 1) indicating the formation of Au nanoparticles in the composite film.

The formations of metallic silver and gold nanoparticles in composites were studied by TEM studies. Fig. 3a and b shows TEM images of Ag and Au nanoparticles embedded composite films. Electron diffraction studies reveal a clear ring pattern for Ag (inset, Fig. 3a) from which the lattice parameter was calculated to be 4.11 Å. This is in good agreement with that of bulk metallic Ag ($a_0 = 4.08$ Å; JCPDS File No. 4-0784). The average particle size of Ag was found to be 16 nm. Fig. 3b shows the TEM micrograph of Au nanoparticles embedded in the composite film.

The formation of highly distributed Au nanoparticles in the composite film with spherical shape can be seen with average particle size of 12 nm. Electron diffraction pattern of Au nanoparticle in Fig. 3b (inset) clearly shows hexagonal diffraction spot pattern, indicating the formation of cubic Au nanoparticles in the composite film. The particle distribution can be altered by changing the concentration of silicotungstic acid in the composite, controlled experiments were demonstrated that the silicotungstate ions are necessary for the rapid reduction of metal nanoparticles in composite films.

Fig. 4a and b shows the XPS spectra of Ag and Au nanoparticles embedded composite films. The obtained binding energy of the Ag 3d and Au 4f were compared with the binding energy values of the respective bulk metal foils. The binding energy values of doublet of Ag $3d_{5/2}$ (368.8 eV), $3d_{3/2}$ (375 eV) and of Au $4f_{7/2}$ (84.1 eV), $4f_{5/2}$ (87.9 eV) are higher than the bulk metal foils. The positive shift in binding energy may be attributed to the size effects of the noble metals in composite films. The positive shift of the BE of nanoparticles with respect to that of bulk metal is consistent with the literature [14].

The formation of Ag or Au nanoparticles in the composite film can be attributed to the transfer of electrons from the reduced silicotungstate ion to Ag^+ or Au^{3+} ions thus leading to zero valent metallic state. Spontaneous self-assembly of silicotungstate anions on Ag(1 1 1) and Ag (1 0 0) are known [15]. We have observed that the formation of Ag nanoparticles is very facile because the diffusion of Ag^+ is higher than that of Au^{3+} and also due to hydrophilic nature of Ag [16]. Upon embedding, the silicotungstate ion in the composite, the first one electron reduction potential is shifted to more negative values. In the composite, the one electron reduction potential of $[\text{SiW}_{12}\text{O}_{40}]^{4-}/[\text{SiW}_{12}\text{O}_{40}]^{5-}$ is -0.096 V versus NHE (parent couple 0.057 V) relative to Ag^+/Ag^0 (0.799 V), $\text{AuCl}_4^-/\text{Au}^0$ (0.99 V). This enhancement in reducing behaviour also favours the facile formation of silver nanoparticles.

Antimicrobial activities of Ag and Au embedded composite films have been investigated against *E. coli* BL 21 as model Gram-negative bacteria. The antimicrobial activities of composite films were carried out by two methods. The first method is disk diffusion method and second is the viable count of bacteria. The first test was performed in Luria–Bertani (LB) medium on solid agar petri dish. The nanoparticle embedded composite film was made into a disc, and was placed on *E. coli* cultured agar plate which was then incubated for 24 h at 310 K and inhibition zone was monitored. It was found that the nanoparticle embedded composite film exhibit an inhibition zone (Fig. 5). In order to see the enhancement of antimicrobial activity, the composite films were dipped in different concentrations of AgNO_3 (5, 20, 40, 70 and 100 mM) for 30 min. It is observed that the diameter of zone of inhibition has increased as the concentration of AgNO_3 is increased (not shown). Similar results have been obtained when the composites are dipped in

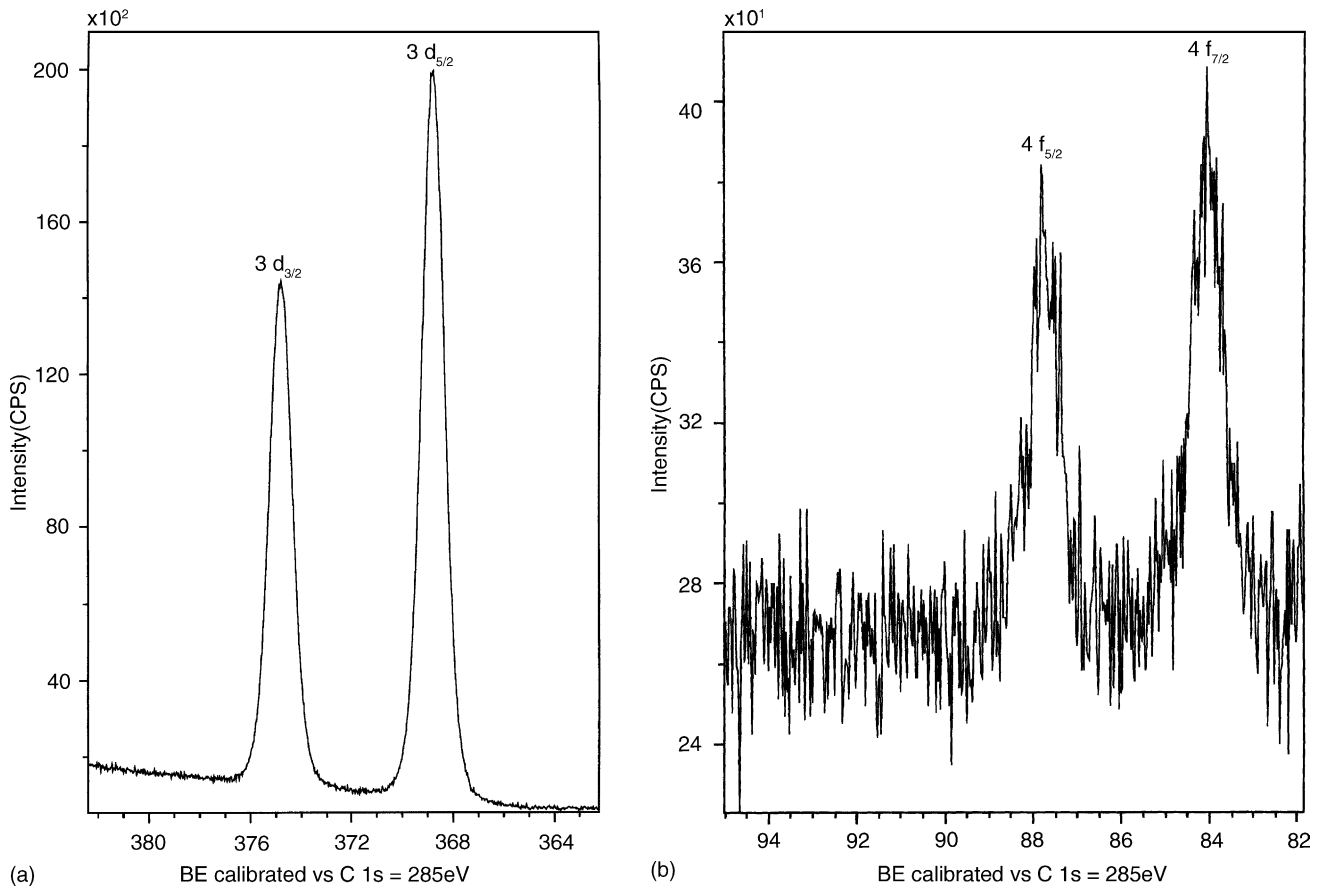


Fig. 4. X-ray photoemission spectra of the core electron binding energy of noble metal nanoparticles embedded composite films: (a) Ag and (b) Au.

different concentrations of HAuCl_4 (3.3 and 5.4 mM). This clearly demonstrates that the antimicrobial activity is only due to noble metal nanoparticles embedded in the composite film and not due to any individual components of the composite. Controlled experiments were carried out with

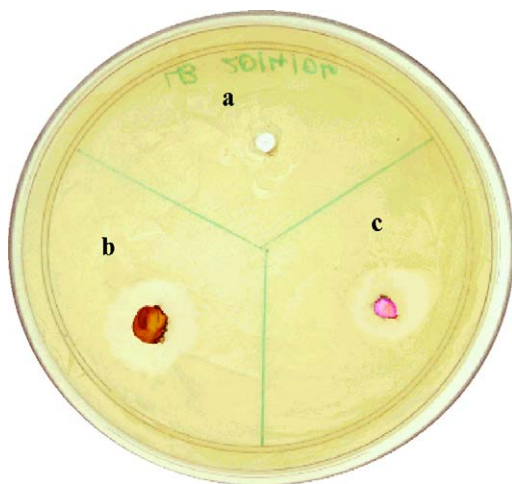


Fig. 5. Antimicrobial activity of noble metal nanoparticles embedded composite films: (a) control (b) Ag and (c) Au.

composite films without metal nanoparticles to corroborate that the antimicrobial activity is only due to the noble metal nanoparticles and not due to any other species present in the composite film. No inhibition zone was observed with the control (Fig. 5a).

The viable bacteria were monitored by counting the number of colony-forming units from the appropriate dilution on nutrient agar plates. The survival fraction was determined calculating the colony-forming units per millilitres of the culture. The activity of the metal composite films after 8 h was examined. It was observed that the silver embedded composite films exhibited the killing rate of *E. coli* to 75% of the viability. For the Au embedded composite film the reductions of viability are 64%. This clearly indicates that the Ag and Au embedded composite films have antimicrobial activities.

The composite can be easily coated onto various substrates and the Ag and Au nanoparticles can be embedded by simple dipping in the respective metal sources. Thus the nanoparticle embedded composite film can be employed in orthopedic materials, urinary catheters, as coating materials and for various commodity products. By proper selection of individual components, these noble metal embedded composite films can be employed in optical filters.

4. Conclusions

In summary, a simple and elegant method is adopted to embed the Ag and Au nanoparticles in organic–inorganic composite film. The sizes of the embedded metal nanoparticles are in the range of 12–16 nm. The nanoparticles embedded composite film exhibits antimicrobial activity against Gram-negative *E. coli*. This demonstrates that the composite film can be employed as environmental friendly antimicrobial surface coating. The presented strategy opens up wide applications in various fields like optical switches, shutters, waveguides, optical filters and in biomedical applications. The adopted synthetic procedure is amenable to fine tune the properties of the composite film by choosing the suitable constituents at molecular level.

References

- [1] S. Forster, M. Antonietti, *Adv. Mater.* 10 (1998) 195; R.P. Adres, J.C. Bielefeld, J.I. Henderson, D.B. Janes, V.R. Kolagunta, C.P. Kubiak, W.J. Mahoney, R.G. Osifchin, *Science* 273 (1996) 1690; M. Moffit, A. Eisenberg, *Chem. Mater.* 7 (1995) 1178; A.P. Alivasatos, *Science* 271 (1996) 933.
- [2] G. Schmid, *Chem. Rev.* 92 (1992) 1709.
- [3] J.D. Holmes, K.P. Johnston, R.C. Doty, B.A. Korgel, *Science* 287 (2000) 1471; E. Braun, Y. Eichen, U. Sivan, G. Ben-Yoseph, *Nature* 391 (1998) 775; A.M. Morales, C.M. Lieber, *Science* 279 (1998) 208; Z.W. Pan, R.Z. Dai, L.Z. Wang, *Science* 291 (2001) 1947; H.Y. Wu, W.P. Qiao, C.T. Chong, X.Z. Shen, *Adv. Mater.* 14 (2002) 64.
- [4] M.T. Pope, *Heteropoly and Isopoly Oxometalates*, Springer, Berlin, 1983.
- [5] A. Troupis, A. Hiskia, E. Papaconstantinou, *Angew. Chem. Int. Ed.* 41 (2002) 1911.
- [6] S. Mandal, P.R. Selvakanan, R. Pasricha, M. Sastry, *J. Am. Chem. Soc.* 125 (2003) 8440; A. Sanyal, M. Murali, *Chem. Commun.* (2003) 236.
- [7] C. Aymonier, U. Schlotterbeck, L. Antonetti, P. Zacharias, R. Thomann, J.C. Tiller, S. Mecking, *Chem. Commun.* (2002) 3018.
- [8] H. Liedberg, T. Lundeberg, *Urol. Res.* 17 (1987) 357–359.
- [9] Y. Zhang, F. Chen, J. Zhuang, Y. Tang, D. Wang, Y. Wang, A. Dong, N. Ren, *Chem. Commun.* (2002) 2814; Y. Zhou, H. Itoh, T. Uemura, K. Naka, Y. Chujo, *Chem. Commun.* (2001) 613; S.K. Mandal, R.K. Roy, A.K. Pal, *J. Phys. D: Appl. Phys.* 36 (2003) 261; L. Yang, G.H. Li, J.G. Zhang, L.D. Zhang, Y.L. Liu, Q.M. Wang, *Appl. Phys. Lett.* 78 (2001) 102; Y. Dirix, C. Bastiaansen, W. Caseri, P. Smith, *J. Mater. Sci.* 34 (1999) 3859; L. Yang, G.H. Li, L.D. Zhang, *Appl. Phys. Lett.* 76 (2000) 1537; G. Mitrikas, C.C. Trapalis, G. Kordas, *J. Chem. Phys.* 111 (1999) 8098; T. He, A. Kunitake, Nakao, *Chem. Mater.* 15 (2003) 4401.
- [10] G.M. Varga, E. Papaconstantinou, M.T. Pope, *Inorg. Chem.* 49 (1970) 662.
- [11] U. Kreibitz, M. Vollmer, *Optical Properties of Metal Clusters*, Springer, Berlin, 1995.
- [12] L.M. Rodriguez-Sanchez, J.F. Rivadulla, M.C. Vergara, M.C. Blanco, M.A. Lopez-Quintela, *J. Phys. Chem. B* 104 (2000) 9683.
- [13] Y.Z. Huang, G. Mills, B. Hajek, *J. Phys. Chem.* 97 (1993) 11542.
- [14] G.K. Wertheim, S.B. Dicenzo, D.N.E. Buchanan, *Phys. Rev. B.* 33 (1986) 5384; G.K. Wertheim, S.B. Dicenzo, S.E. Youngquist, *Phys. Rev. Lett.* 51 (1983) 2310; H.S. Shin, H.C. Choi, Y. Jung, S.B. Kim, H.J. Song, H.J. Shin, *Chem. Phys. Lett.* 383 (2004) 418.
- [15] M. Ge, B. Zhong, W.G. Klemperer, A.A. Gewirth, *J. Am. Chem. Soc.* 118 (1996) 5812; L. Lee, J.X. Wang, R.R. Adzic, I.K. Robinson, A.A. Gewirth, *J. Am. Chem. Soc.* 123 (2001) 8838.
- [16] G.W. Arnold, J.A. Borders, *J. Appl. Phys.* 48 (1977) 1488.